A Fully Micromachined W-Band Coplanar Waveguide to Rectangular Waveguide Transition

Yuan Li, Bo Pan, Manos. M.Tentzeris and John Papapolymerou

GEDC, School of Electrical & Computer Engineering, Georgia Institute of Technology, Atlanta, GA 30332

Abstract— **A novel fully micromachined coplanar waveguide (CPW) to rectangular waveguide transition is presented in this paper. A metalized probe is adopted to couple the signal from the CPW to the rectangular waveguide through an aperture located at the center of the bottom broad wall of the rectangular waveguide. The transition was optimized using HFSS 10 over the whole W-band. In the proposed transition, the CPW and the rectangular waveguide are patterned and integrated on the same side of the substrate, while the coupling probe is patterned on the substrate instead of being fabricated separately. These changes make the transition more suitable for RF packaged circuits and easily extendable to THz applications. The measured average insertion loss of the back-to-back structure is 2.25dB and the return loss is better than 11 dB over the whole W-band.**

Index Terms— **Micromachining, rectangular waveguide, Coplanar waveguide, Transition, Deep reactive ion etching, W-band**

I. Introduction

Fueled by the demand of compact monolithic microwave integrated circuits (MMICs) for telecommunication and space applications, significant amount of research has been performed on coplanar waveguide (CPW) based topologies due to CPW's several advantages over other competing transmission lines [1,2]: The grounds and the signal are on the same side of the substrate eliminating the need for via-holes or wraparound process [3,4]. Also, the characteristic impedance is determined by the ratio of the width of center strip conductor to the distance between the two semi-infinite ground planes [5] enabling compact designs, something demonstrated by the numerous CPW-based microwave probes commonly used for the characterization of microwave integrated circuits.

Rectangular waveguides, on the other hand, have the advantages of low loss and high power handling capacity. However, the traditional rectangular waveguides at low frequencies are bulky making almost impossible their integration into system-on-chip geometries. Nevertheless, the size of rectangular waveguides shrinks dramatically at or above the mm-wave frequency range or even in Terahertz frequencies [6]-[8]. At the same time, the losses of other transmission lines, such as microstrips, keep increasing when the frequency goes up.

Various transitions from CPW to rectangular waveguide have been proposed in the past, in order to combine their respective advantages. Either a ridge and a non-radiating slot, located at opposite sides of the broad wall of the rectangular waveguide [9] or a ridge and a trough [10], are introduced to convert the waveguide TE_{10} mode into the CPW field. In [11], two transitions, the post coupler and the slot coupler, are demonstrated and in [12] fully micromachined transitions are shown using the probes on finite-ground coplanar line.

This paper presents a novel fully micromachined CPW to rectangular waveguide transition. Compared to [9, 10], the proposed transition has the advantage of easier mass production by using the silicon micromachining technique. The CPW and the rectangular waveguide are patterned and integrated on the same side of the substrate in this paper instead of the both sides of the substrate [11]. Plus, the coupling probe is patterned on the substrate instead of being fabricated separately [12]. The proposed transition doesn't need the probe assembly like [12]. These changes make the transition more suitable for RF packaged circuits and easily extendable to THz applications.

II. Transition Design and Simulation

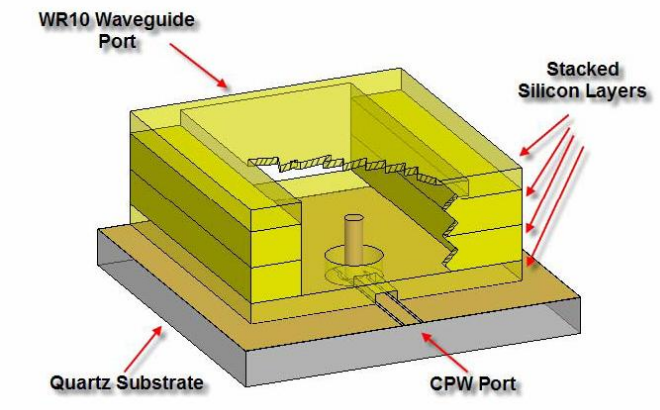

Fig. 1. The schematic diagram of the transition.

This on-wafer CPW to rectangular waveguide transition is composed of two parts: a CPW to vertical probe part and a probe to waveguide part, as shown in Fig. 1. The CPW line is patterned on the top of the quartz substrate and is first terminated into a vertical probe [13], which is then inserted into the waveguide through its bottom broad wall. The micromachined waveguide is mounted on top of the quartz substrate (diel.constant 3.78), with a rectangular slit etched to feed the CPW in. The whole rectangular waveguide is made by four silicon layers, which are stacked and aligned together [14].

Contrary to previous approaches, in this paper the CPW line is fabricated on the top of the quartz glass with 1.5mm thickness. The vertical coupling probe is patterned on the quartz substrate. The impedance of the coaxial structure formed by the probe and the metalized silicon hole is provided by:

$$Z_c = \frac{1}{2\pi}\left(\frac{\mu_0}{\varepsilon'}\right)^{1/2} \ln\frac{R2}{R1} \qquad (1)$$

where, μ_0 is the permeability of the vacuum, ε' is the real permittivity and R2 and R1 are the radii of the aperture and the probe, respectively. The impedance of the coaxial structure is selected to match the impedance of the CPW. However, the parasitics caused by the discontinuity of circular aperture and the circular tapering of the CPW ground around probe is one of the reasons that cause the mismatching in the measurement of return loss.

The standard WR-10 waveguide dimensions (2.54mm x 1.27mm) are utilized for the rectangular waveguide. The silicon layer on the bottom is patterned on a 300um thick wafer. The CPW line is fabricated on the top of a 1.5mm thick quartz substrate. The CPW beyond the probe is terminated in a short-stub for achieving a good impedance matching. The probe is located in the center of the broad wall. The design of transition from probe to waveguide is based on matching the coaxial structure with probe to waveguide. The distance from probe to backshort (L in Fig.2), the height of the probe and the radius of the probe are critical in the matching. Finally, the transition is optimized using the full-wave simulator, HFSS, leading to the dimensions, shown in Fig. 2 and listed in Table 1, while the optimized insertion loss and return loss of the transition are shown in Fig. 3.

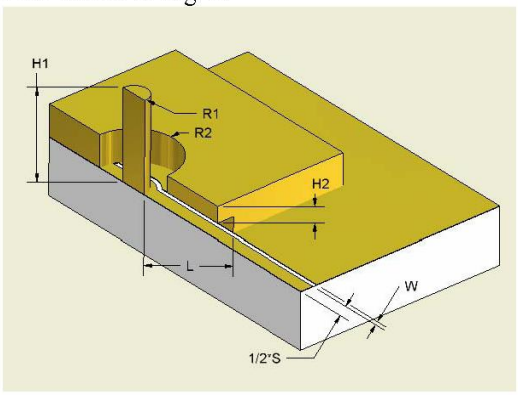

Fig. 2. The CPW and the coupling probe (The transition is shown in half from the center of the broad wall due to its symmetry, the metalized silicon sidewalls with thickness T are not shown).

Table 1. The dimensions of the transition

Dimensions	Value(um)
H1	850
H2	150
R1	115
R2	400
W	40
S	240
L	885

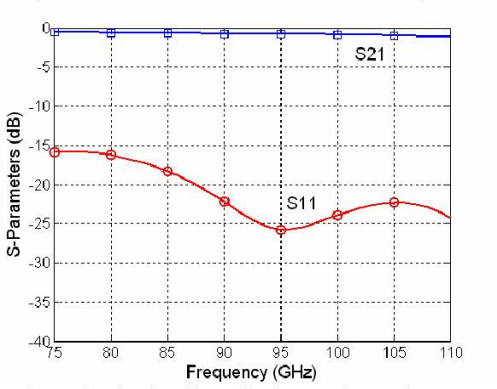

Fig. 3.The simulated insertion loss and return loss.

To facilitate the measurement, the transition structure is fabricated in a back-to-back configuration that is shown in Fig. 4. The optimized simulation of the back-to-back transition is provided in Fig. 5. The simulated insertion loss of the back-to-back structure is between 0.87 dB and 2.68 dB over W-band (75-110GHz).

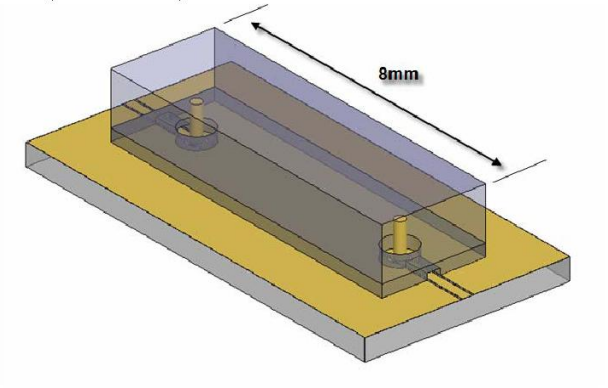

Fig. 4. The back-to-back structure.

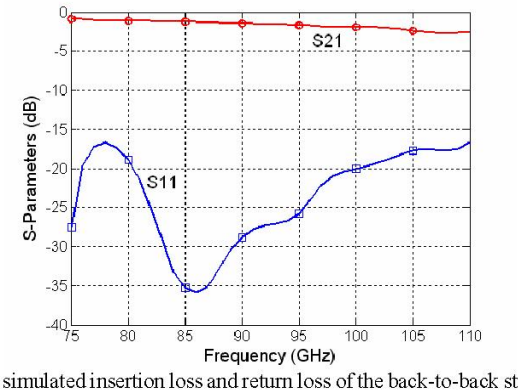

Fig. 5.The simulated insertion loss and return loss of the back-to-back structure.

III. Fabrication

A. Fixture

A fixture, shown in Fig. 6(a), was designed to facilitate the alignment. The alignment pins were applied on the base of the fixture and provided the reference to align the silicon parts and helped to snap them together.

B. Stacked substrates

Four silicon layers were fabricated using the deep reactive ion etching (DRIE) technique. The bottom layer was made by a 300um thick silicon wafer. The aperture was patterned on this wafer. The two middle layers were fabricated using the 525um thick wafers. The top layer was etched only 220um deep with the pattern of the rectangular waveguide and released from the back. Finally, the four silicon layers formed a rectangular waveguide with a 1.27mm height. The metalized probe was fabricated on the 1.5mm quartz substrate as well as the CPW line. A picture of the fixture and the stacked samples were shown in Fig. 6.

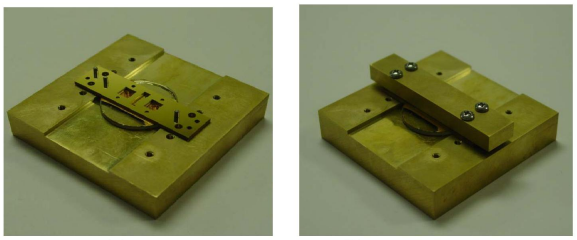

(a) (b)

Fig. 6. (a) The fixture, quartz substrate and the silicon layers. (b) The whole transition with fixture.

C. Fabrication flow of the Silicon wafer

The first step of the silicon substrate preparation was wafer cleaning. Then, photoresist(PR) SRP220 was spun and patterned on the topside of the silicon wafer. The patterned wafer was baked at 115 degrees for 5 minutes, before the STS ICP was applied to etch the topside to the desired depth. A clean process was utilized to clean the remaining PR from the topside etching. Then, the Uniaxis PECVD was used to deposit a thin silicon dioxide layer to protect the patterned topside. Once the silicon dioxide was deposited, the wafer was flipped and patterned using the PR on the backside. Then, the sample was released by using the backside etching. Finally, BOE was applied to remove the silicon dioxide layer. The silicon samples were metallized using DC-Sputter with Ti/Cu/Au. The fabrication flow was shown in Fig. 7-1.

D. Fabrication flow of the feeding CPW and the probe

The Ti/Cu/Ti layer was sputtered and patterned to open the window for the SU-8 patterning from the backside of the transparent quartz wafer. This improves the SU-8 adhesion to the quartz. An 800 µm negative photo-definable epoxy SU-8 2035 was dispensed uniformly on the top of the glass. It was patterned under UV to define the mold of the vertical probe. Another Ti/Cu/Ti was sputtered as the seed layer to cover the probes, as well as the substrate in a conformal manner. Then, the negative photo-resist NR9-8000 was coated and patterned in a non-contact way to cover the CPW slot region, preventing the metal coverage on the slot in the following electroplating step. 6µm copper and 2µm gold were electroplated to cover the sidewall of the probe, as well as the exposed ground feeding structures. As the final step, the photo-resist NR9-8000, as well as the seed layer were removed one by one to release the structure. The fabrication flow is shown in Fig. 7-2. Fig.8 gives the SEM picture of the probe and the aperture on the 300um thick wafer.

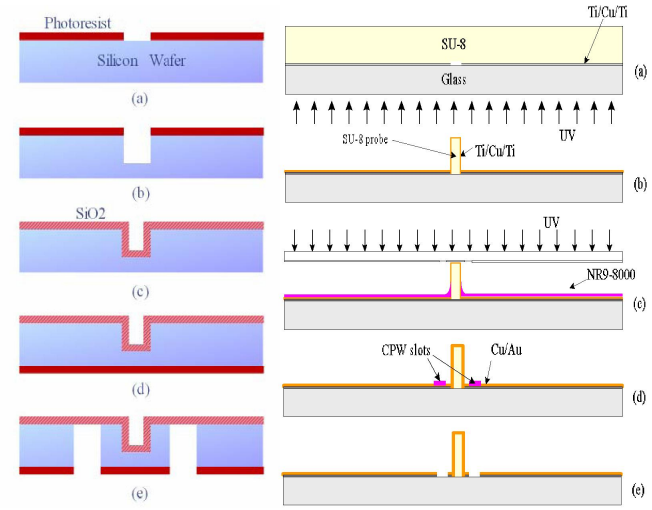

Fig. 7-1 Fig.7-2

Fig. 7. (1) The fabrication flow of silicon rectangular waveguide. (2). The fabrication flow of CPW and Probe

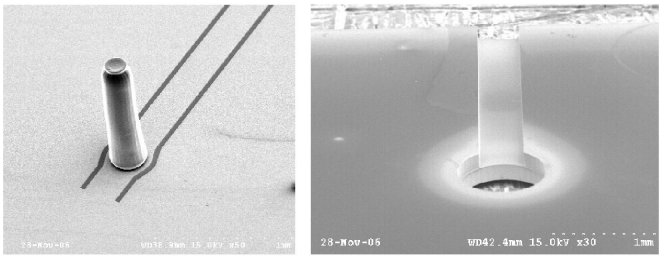

Fig. 8. (a) The probe and CPW. (b) The aperture on the 300um thick wafer.

IV. Measurement

The S-parameters measurements of the waveguide transition were taken by using Agilent Vector Network Analyzer 8510XF. The NIST Multical TRL algorithm was used to calibrate the measurement system by using the HP BASIC. The insertion loss and the return loss of the back-to-back structure are reported in Fig. 9. The measured average insertion loss of the back-to-back structure is 2.25dB with about 1dB ripple and the return loss is better than 11 dB over the whole W-band. Compared to the simulation in Fig. 5, the return loss is still higher than simulated return loss due to the tolerance in the fabrication.

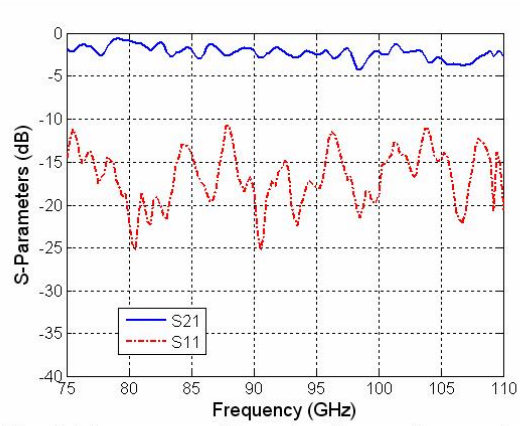

Fig. 9. The measured insertion loss and return loss.

V. Conclusion

In this paper, a novel fully micromachined coplanar waveguide (CPW) to rectangular waveguide transition is presented. In the proposed transition, the CPW and the rectangular waveguide are patterned and integrated on the same side of the substrate, while the coupling probe is patterned on the substrate instead of being fabricated separately. These changes make the transition more suitable for RF packaged circuits and easily extendable to THz applications. The simulated insertion loss of the back-to-back structure is between -0.87 dB and -2.68 dB and simulated return loss is less than -16.6 dB over the W-band. The measured average insertion loss of the back-to-back structure is 2.25dB and the return loss is better than 11 dB over the whole W-band.

Acknowledgements

This work is partially supported by an NSF CAREER grant and partially supported by an ARO Young Inv. Award. The authors wish to thank the support from Dr. Guoan Wang, Pete Kirby and the Georgia Electronic Design Center.

References

[1] N. I. Dib, M. Gupta, G. E. Ponchak, and L. P. B. Katehi, "Characterization of asymmetric coplanar waveguide discontinuities," IEEE Trans.Microwave Theory Tech., vol. 41, pp. 1549–1558, Sept. 1993.

[2] C. P. Wen, "Coplanar Waveguide: A Surface Strip Transmission Line Suitable for Nonreciprocal Gyromagnetic Device Applications," *IEEE Trans. Microwave Theory Tech.*, Vol. 17, No. 12, pp. 1087—1090, Dec. 1969.

[3] J. Browne, "Broadband Amps Sport Coplanar Waveguide," *Microwaves RF*, Vol. 26, No. 2, pp. 131—134, Feb. 1987.

[4] J. Browne, "Coplanar MIC Amplifier Bridges 0.5 To 18.0 GHz," *Microwaves RF*, Vol. 26, No. 6, pp. 194—195, June 1987.

[5] Rainee N. Simons, Coplanar Waveguide Circuits, Components, and Systems, New York, John Wiley & Sons, Inc., 2001

[6] Q. Xiao, Y. Duan, J. L. Hesler, T. W. Crowe and R. Weikle II, "A 5-mW and 5% efficiency 210 GHz InP-based heterostructure barrier varactor quintupler," *IEEE Microwave and Wireless Components Letters*, pp. 159-161, April 2004.

[7] A. Maestrini, J. S. Ward, J. J. Gill, H. S. Javadi, E. Schlecht, C. Tripon-Canseliet, G. Chattopadhyay, I. Mehdi, "A 540-640-GHz high-efficiency four-anode frequency tripler," *IEEE Trans. Microwave Theory Tech.*, Vol. 53, No. 9, pp. 2835 - 2843, Sep. 2005.

[8] P. L. Kirby, D. Pukala, H. Manohara, I. Mehdi, J. Papapolymerou, "Characterization of micromachined silicon rectangular waveguide at 400 GHz," *IEEE Microwave and Wireless Components Letters*, pp. 366-368, June 2006.

[9] G. E. Ponchak and R. N. Simons, "A New Rectangular Waveguide to CoplanarWaveguide Transition," *IEEE MTT-S Int. Microwave Symp.* Dig., Dallas, TX, Vol. 1, pp. 491-492, May 8-10, 1990

[10] E. M. Godshalk, "A V-Band Wafer Probe Using Ridge-Trough Waveguide," *IEEE Trans. Microwave Theory Tech.*, Vol. 39, No. 12, pp. 2218—2228, Dec. 1991.

[11] R. N. Simons, "New Channelized Coplanar Waveguide to Rectangular Waveguide Post and Slot Couplers," *Electron. Letter*, Vol. 27, No. 10, pp. 856—857, May 1991.

[12] Y. Lee, J. P. Becker, J. R. East, and L. P. B. Katehi, "Fully micromachined finite-ground coplanar line-to-waveguide transitions for W-band applications," *IEEE Trans. Microw. Theory Tech.*, vol. 52, no. 3, pp. 1001–1007, Mar. 2004.

[13] B. Pan, Y. Yoon, P. Kirby, J. Papapolymerou, M. M. Tentzeris and M.Allen, "A W-band Surface Micromachined Monopole for Low-cost Wireless Communication Systems", *IEEE-IMS Symposium*, pp.1935-1938, Fort-Worth, TX, June 2004

[14] Y. Li, P. L. Kirby, "Silicon Micromachined W-Band Bandpass Filter Using DRIE Technique", Accepted 2006 *European Microwave Conference*, pp.1271-1273, Manchester, UK, September 2006